Cellular/Molecular

The Reelin Signaling Pathway Promotes Dendritic Spine Development in Hippocampal Neurons

Sanyong Niu,[1,2]* **Odessa Yabut,**[3,4]* **and Gabriella D'Arcangelo**[4]

[1]The Cain Foundation Laboratories, Texas Children's Hospital, Houston, Texas 77030, [2]Department of Pediatrics and [3]Program in Developmental Biology, Baylor College of Medicine, Houston, Texas 77030, and [4]Department of Cell Biology and Neuroscience, Rutgers, The State University of New Jersey, Piscataway, New Jersey 08854

The development of distinct cellular layers and precise synaptic circuits is essential for the formation of well functioning cortical structures in the mammalian brain. The extracellular protein Reelin, through the activation of a core signaling pathway, including the receptors ApoER2 and VLDLR (very low density lipoprotein receptor) and the adapter protein Dab1 (Disabled-1), controls the positioning of radially migrating principal neurons, promotes the extension of dendritic processes in immature forebrain neurons, and affects synaptic transmission. Here we report for the first time that the Reelin signaling pathway promotes the development of postsynaptic structures such as dendritic spines in hippocampal pyramidal neurons. Our data underscore the importance of Reelin as a factor that promotes the maturation of target neuronal populations and the development of excitatory circuits in the postnatal hippocampus. These findings may have implications for understanding the origin of cognitive disorders associated with Reelin deficiency.

Key words: reeler; Dab1; VLDLR; ApoER2; synapse; postsynaptic

Introduction

A late step in neuronal maturation, which occurs mostly at postnatal ages, consists of synapse formation and the establishment of connectivity. Synaptogenesis is the result of a complex series of events that includes the acquisition of synaptic competence and the apposition of presynaptic and postsynaptic anatomical structures (Craig et al., 2006). A variety of secreted or cell adhesion proteins have been implicated in the genesis of excitatory or inhibitory synapses, but much remains to be understood about this important process at the molecular level.

In recent years the extracellular protein Reelin has emerged as an important factor that affects several steps in brain development, from neuronal migration to dendritogenesis and synaptic transmission. Homozygous *reeler* mice lacking Reelin are severely ataxic and exhibit disrupted cellular layers and dendritic trees in neocortical, hippocampal, and cerebellar structures (for review, see Lambert de Rouvroit and Goffinet, 1998; D'Arcangelo, 2006). Heterozygous *reeler* mice, however, appear normal, but dendrite development is delayed (Niu et al., 2004) and the mice are impaired in at least some tests of cognitive function (Tueting et al.,

1999; Niu et al., 2004; Brigman et al., 2006; Krueger et al., 2006). The activity of Reelin in layer formation and dendritogenesis is mediated by the same basic signaling pathway, consisting of two Reelin receptors [ApoER2 and very low density lipoprotein receptor (VLDLR)], src-family kinases (SFKs) Src and Fyn, and the adapter protein Disabled-1 (Dab1) (for review, see D'Arcangelo, 2006). Homozygous mice lacking ApoER2 and VLDLR (Trommsdorff et al., 1999), Src and Fyn (Kuo et al., 2005), or Dab1 (Howell et al., 1997; Sheldon et al., 1997; Ware et al., 1997), like *reeler*, exhibit ataxia, disruption of cortical cellular layers, and impaired dendrite development (Tabata and Nakajima, 2002; Niu et al., 2004; Olson et al., 2006; Maclaurin et al., 2007).

Previous anatomical studies of mutant mice revealed that Reelin is important for the development of precise synaptic connectivity in the cerebellum (Mariani, 1982), hippocampus (Borrell et al., 1999), and retina (Rice et al., 2001). However, these defects appeared to arise from improper pruning or branching of presynaptic axonal fibers, or from an indirect deficit in neuron survival. A more direct role for Reelin in the modulation of synaptic function in the brain has been appreciated in recent years (for review, see D'Arcangelo, 2005; Herz and Chen, 2006). These studies demonstrate that Reelin affects synaptic strength and plasticity. However, it is not yet known whether the Reelin pathway directly affects the formation or the stabilization of anatomical synapses during development.

In this study we investigated the effect of the Reelin pathway on the development of postsynaptic structures in hippocampal glutamatergic synapses. Dendritic spines in apical dendrites of fluorescently labeled hippocampal pyramidal neurons were analyzed *in vivo* and in organotypic cultures by confocal microscopy. The expression and the recruitment of postsynaptic proteins to hippocampal synaptosomes were also examined by biochemical

assays. We demonstrate for the first time a direct role of the canonical Reelin pathway in the formation or stabilization of dendritic spines in the postnatal hippocampus.

Materials and Methods

Reagents. Cell culture medium and reagents were purchased from Invitrogen. G10, a mouse monoclonal antibody against Reelin, was purified from hybridoma cell culture supernatants using Hi-Trap protein G columns (GE Healthcare). Glutathione *S*-transferase–receptor-associated protein (GST-RAP) was prepared as described previously (Niu et al., 2004). PP2 and PP3 were from Calbiochem. Antibodies used were rabbit anti-Dab1 (Rockland Immunochemicals), rabbit anti-synaptophysin (Synaptic Systems), mouse anti-actin (Millipore Bioscience Research Reagents), mouse anti-PSD-95 (postsynaptic density protein 95) (Millipore Bioscience Research Reagents), rabbit anti-NR2A (Millipore Bioscience Research Reagents), and mouse anti-synapsin IIA (BD Transduction Laboratories, BD Biosciences). Reelin was obtained as the conditioned medium of the stable cell line CER (Niu et al., 2004). Mock medium was prepared from the parental human embryonic kidney 293-EBNA (Epstein-Barr virus nuclear antigen) cell line. Both media were concentrated ~30-fold by centrifugation using Amicon Ultra filters (Millipore) at $2680 \times g$ for 20 min before addition to neuronal cultures.

Mouse colonies. All of the experiments were performed in accordance with procedures approved by the Animal Protocol Review Committee of Baylor College of Medicine and Rutgers according to national and institutional guidelines for animal care established by the National Institutes of Health and approved by the competent Animal Ethics Committee. *reeler* mice (B6C3Fe-*a/a-Relnrl/*+) were obtained from The Jackson Laboratory and genotyped by PCR using the following primers: forward, TAATCTGTCCTCACTCTGCC; reverse wild-type, ACAGTTGACAT-ACCTTAATC; and reverse *reeler*, TGCATTAATGTGCAGTGTTG. PCR conditions were as follows: 1 cycle, 5 min at 94°C; 30 cycles, 1 min at 94°C, 2 min at 55°C, 3 min at 72°C; 1 cycle, 10 min at 72°C. *Thy1-YFP* transgenic mice (B6.Cg-TgN(Thy1-YFPH)2Jrs) were obtained from The Jackson Laboratory and genotyped by PCR as suggested by the distributor. *Dab1* knock-out mice were obtained from J. A. Cooper (Fred Hutchinson Cancer Research Center, Seattle, WA) and genotyped as described previously (Howell et al., 1997). Heterozygous *reeler* or heterozygous *Dab1* knock-out mice were crossed with *Thy1-YFP* transgenic mice to generate the *reeler-YFP* or *Dab1* knock-out-*YFP* mouse colonies, respectively.

Hippocampal organotypic culture and treatments. Hippocampal cultures were prepared essentially as described previously (Stoppini et al., 1991) from wild-type, heterozygous, and homozygous *reeler* littermates or wild-type, heterozygous, and homozygous *Dab1* knock-out littermates expressing the *YFP* transgene. The hippocampi were dissected at postnatal day 4 (P4) and placed in Leibovitz's L-15 media. Meningeal membranes were pealed off and the tissues were placed on the stage of a custom-built tissue chopper. Transverse slices (375 μm thick) were cut and placed on Millicell (Millipore) membranes soaked in culture medium containing 98% Neurobasal-A, 2% B-27 supplement, and 0.5 mM glutamine. Typically six to seven slices were cultured on one membrane and maintained at 37°C in 5% CO_2 in a water-jacked incubator. Culture medium was changed every other day. Sister cultures from the same animal were treated with various agents or left untreated for 11 d *in vitro*. Chronic treatment of slices was started on the day after dissection and was maintained by adding 30× concentrated mock or Reelin conditioned medium (containing ~100 ng/ml Reelin), 50 μg/ml GST-RAP, 50 μg/ml GST, 5 μM PP2, or 5 μM PP3. Experiments were terminated by fixation in fresh 4% paraformaldehyde. A blind code was then assigned to each culture dish by a different experimenter before imaging acquisition and analysis.

Immunofluorescence and immunohistochemistry. Fixed organotypic cultures (375 μm thick) were lifted from membrane inserts with a fine artist paintbrush and kept free-floating in PBS. Free-floating sections (40 μm thick) were also prepared from the brain of *reeler-YFP* and *Dab1* knock-out (*Dab1*KO)-*YFP* mice perfused at P21 or P32. All sections were blocked in PBS containing 0.25% Triton X-100 and 5% normal goat

serum for 1 h, incubated overnight at 4°C with primary antibodies, and then incubated for 1 h with secondary antibodies Alexa 594 goat anti-rabbit or Alexa 594 goat anti-mouse IgG (Invitrogen) for immunofluorescence. To visualize yellow fluorescent protein (YFP) fluorescence, the sections were directly imaged by confocal microscopy using a FluoView FV300 (Olympus) or an LSM 510 Meta (Zeiss) confocal laser scanning microscope. Some brain sections were also processed for anti-GFP immunohistochemistry using the Vectastain Elite ABC kit (Vector Laboratories), and the signal was detected by 3,3'-diaminobenzidine substrate (Vector Laboratories). To measure the extension of apical dendrites, YFP-labeled pyramidal neurons in the CA1 region of hippocampal tissue sections obtained from wild-type and heterozygous *reeler* mice were imaged using an Olympus IX50 fluorescence microscope. The length of apical projections from the pyramidal layer to the bottom of the stratum lacunosum molecular (SLM) was measured using the NIH Image J software. A total of five sections were analyzed for each genotype, and three measurements were obtained from each section. Student's *t* test was used for statistical analysis.

Tracing and analysis of dendritic spines. YFP-labeled dendrites in 375-μm-thick organotypic cultures or 40-μm-thick brain sections were imaged using confocal microscopy. For quantitative analysis, apical dendritic segments 20–40 μm long in the stratum radiatum (SR) and SLM were imaged using the FluoView FV300 confocal microscope and a 60× UPlanApo objective (numerical aperture = 0.65–1.25) (Olympus) followed by 3× digital zoom. Kalman accumulation at an average of 2 was used to reduce noise. Maximum projection images were generated from 0.15 μm incremental steps in the z-axis. Apical dendrites could be readily identified in wild-type and heterozygous *reeler* or *Dab1* knock-out mice based on their stereotypical projections. For homozygous mutant sections in which pyramidal neurons appeared disorganized and disoriented, apical dendrites were tentatively identified based on their relatively longer extension compared with basal branches. Dendritic branches were classified as second to fourth order according to their topological centrifugal order, in which branch order starts at 1 for branches connected to the soma and increases after each branch point. Primary dendrites were not included in the analysis. Terminal branches that could not be traced to the soma but that exhibited a terminal tip were analyzed separately from second- to fourth-order branches. These may include cut ends and do not necessarily correspond to the most distal branches. Dendritic spines were scored only if they exhibited a distinct morphology defined as the presence of a neck and a mushroom-shaped or thin-shaped head. These types of spines were by far the most abundant protrusions observed in P21/P32 mouse brain sections or 11 day in *vitro* (DIV) culture slices. Stubby protrusions, at which neck and head structures could not be distinguished, or filopodia were not included in the analysis. Spines were quantified from confocal image projections of dendritic segments traced with a digital Neurolucida using the NeuroExplorer software (MBF Bioscience). The data in each experimental or control sample were obtained from 25 to 35 dendritic segments of multiple neurons from multiple sections or slices. All dendritic segments were analyzed in blind with respect to the genotype or the treatment received in each experimental group. Each type of experiment was repeated three times, and the results were combined for final analysis. Student's *t* test was used to determine statistical significance ($p < 0.05$).

Protein extracts and crude synaptosome preparation. The hippocampi of P21 or P32 wild-type, heterozygous, and mutant littermates were processed for synaptosome fractionation at the same time. The tissue was dissected in 0.9% NaCl and placed in 500 μl of ice-cold homogenization buffer containing 0.32 M sucrose, 1 mM EDTA, 5 mM HEPES, pH 7.4, and protease inhibitor Complete Mini tablet (Roche) for homogenization (Glas-Col homogenizer, Thomas Scientific). Total lysates were centrifuged at $800 \times g$ for 10 min at 4°C. The supernatant was collected and centrifuged again at $800 \times g$ for 10 min at 4°C. The supernatant was collected and subjected to a third centrifugation at $7200 \times g$ for 15 min at 4°C. The pellet, containing the synaptosome fraction, was resuspended in 100 μl of homogenization buffer. The protein concentration of the total lysates as well as the synaptosome fractions were measured and normalized with homogenization buffer.

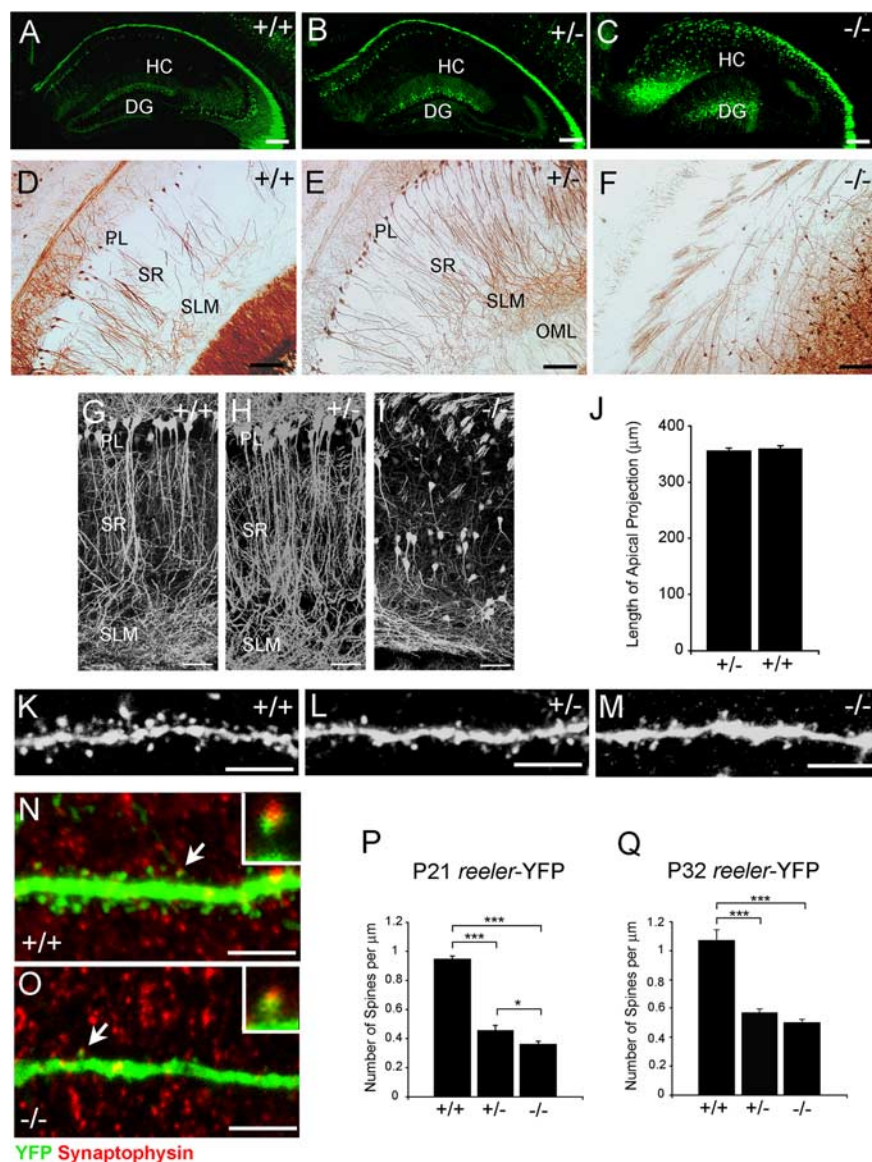*Western blot analysis.* Total lysate or synaptosome fractions (10 μg)

Figure 1. Dendritic spine density is reduced in hippocampal pyramidal neurons of heterozygous and homozygous *reeler* mice. *A–C*, Low-magnification confocal images of the hippocampus of adult wild-type, heterozygous, or homozygous *reeler-YFP* littermates. YFP-positive neurons are ectopic in homozygous *reeler* mice. Scale bars, 200 μm. *D–F*, YFP immunohistochemistry in floating sections of wild-type, heterozygous, or homozygous *reeler-YFP* littermates. Scale bars, 100 μm. *G–I*, Composite confocal images of CA1 apical projections of adult wild-type, heterozygous, or homozygous *reeler-YFP* littermates. YFP-positive pyramidal neurons appear normal in heterozygous mice, whereas they are stunted and misoriented in homozygous *reeler* mice. Scale bars, 50 μm. *J*, Quantification of the extent of the apical projection in wild-type and heterozygous *reeler* mice reveal no difference between these genotypes. *n* = 15 measurements per genotype. Bar graphs show the mean ± SEM. *K–M*, High-magnification representative confocal images of second-order apical dendrite branches of CA1 pyramidal neurons. Mature spines are present in all genotypes. Scale bars, 5 μm. *N–O*, Confocal images of wild-type or *reeler* mutant YFP-positive dendrites double labeled with synaptophysin antibodies. The insets show enlarged images of the synapses indicated by the arrows. Scale bars, 5 μm. *P–Q*, Quantification of spine density in second- to fourth-order apical dendrite branches in P21 (*P*) or P32 (*Q*) mice. Spine density is significantly reduced in heterozygous and homozygous *reeler* compared with wild-type mice at both ages. *n* = 25 dendrite segments per genotype from three independent experiments. Bar graphs show the mean ± SEM; **p* < 0.03; ***p < 0.001. HC, hippocampus proper; DG, dentate gyrus; PL, pyramidal layer.

were loaded in 4–12% Tris-glycine SDS-polyacrylamide gels (Invitrogen), separated at 120 V for 2 h, and transferred to 0.22 μm nitrocellulose membrane (Invitrogen) at 200 mA for 2 h. The membranes were blocked with 3% milk/1× TBS-T (Tris-buffered saline with 0.1% Tween 20) for 1 h at room temperature followed by incubation with primary antibodies, and then secondary antibodies diluted in 0.3% milk/1× TBS-T for 1 h at room temperature. Membranes were washed three to four times in 1× TBS-T for 1 h, incubated with ECL-Plus Western Blotting Detection

System (GE Healthcare Bio-Sciences) for 5 min, and exposed to autoradiographic film (Denville Scientific). X-ray films were scanned for densitometry analysis using NIH ImageJ software. The percentage change of the protein levels in heterozygous or mutants from wild-type synaptosome fractions was measured. Student's *t* test was used for statistical analysis.

Results

Reelin deficiency results in a reduced density of spines on apical dendrites of hippocampal pyramidal neurons

In the embryonic and early postnatal hippocampus, Reelin is expressed at high levels by Cajal-Retzius cells, which secrete large amounts of the protein in the SLM of the hippocampus proper and in the outer marginal layer of the dentate gyrus (D'Arcangelo et al., 1995; Alcántara et al., 1998). GABAergic interneurons in all layers of the hippocampus also begin to express Reelin at early postnatal ages but persist throughout adult life, whereas Cajal-Retzius cells slowly disappear. Components of the Reelin signaling pathway such as ApoER2, VLDLR, and Dab1 are expressed throughout development in hippocampal pyramidal and dentate gyrus neurons (Trommsdorff et al., 1999; Niu et al., 2004).

To investigate the development of dendritic spines in Reelin target cells, we took advantage of a transgenic mouse line expressing YFP in selected neuronal populations under the control of the *Thy1* promoter (line H) (Feng et al., 2000). In this line, high levels of YFP expression are observed in the hippocampus starting from the second postnatal week and are maintained throughout adulthood in some pyramidal neurons in areas CA1 and CA3, and in many dentate gyrus neurons. We bred these transgenic mice with *reeler* heterozygous mice to generate a *reeler-YFP* colony and then crossed heterozygous mice to obtain YFP-positive wild-type, heterozygous, and homozygous *reeler* mice for our study. When hippocampal sections from P21 mice were examined by fluorescence confocal microscopy, YFP-positive neurons appeared to be normally placed in the pyramidal layer of wild-type and heterozygous *reeler* mice, but they were clearly ectopic in homozygous *reeler* mutants, as expected (Fig. 1*A–C*). To study spine development, we focused on apical dendrites of CA1 pyramidal neurons because the limited number of YFP-positive processes facilitates their analysis, and also because they project toward the Reelin-rich SLM and thus are more likely to be affected by this protein. The overall length and orientation of the apical tree of YFP-positive CA1 pyramidal neurons appeared normal in wild-type (Fig. 1*D*) and heterozygous *reeler* mice (Fig. 1*E*), whereas these projections were obviously misoriented and stunted in ho-

mozygous *reeler* mutants (Fig. 1*F*). To examine apical dendrites in more detail, we collected composite, high-resolution confocal stack images of YFP-labeled projections in comparable CA1 regions of wild-type, heterozygous, and homozygous *reeler* mice (Fig. 1*G–I*). These images confirmed that apical dendrites appear morphologically normal in heterozygous mice, whereas they are severely reduced in length and complexity in homozygous *reeler* mice. Quantitative analysis of the thickness of the apical projection, defined as the distance between the pyramidal layer and the hippocampal fissure, further demonstrated that the extension of apical dendrites is similar in wild-type and heterozygous mice (Fig. 1*J*). We then analyzed second- to fourth-order and terminal apical branches of YFP-positive pyramidal neurons in the SR and SLM to determine whether they bear dendritic spines. When dendritic segments from P21 mice were imaged at high magnification by confocal microscopy, mature dendritic spines with distinct neck and head morphology were readily observed in all genotypes (Fig. 1*K–M*; supplemental Fig. 1*A–C*, available at www.jneuro-sci.org as supplemental material). Double labeling with antibodies against the presynaptic marker synaptophysin revealed that axon terminals were juxtaposed to at least some YFP-labeled spines in both wild-type and mutant dendrites, indicating that these latter structures can participate in the formation of synapses (Fig. 1*N,O*). However, in this study, we focused on the effect of Reelin on the development of postsynaptic components of the synapse defined as YFP-labeled, mushroom-shaped spine protrusions, and not that of the synapse as a whole. Quantitative analysis indicated that the density of spines was dramatically and significantly reduced in heterozygous and homozygous *reeler* mutants compared with wild-type mice ($p < 0.001$). Values in the second- to fourth-order branches were (spines/μm): wild type, 0.94 ± 0.02; heterozygous, 0.46 ± 0.03; and mutant, 0.36 ± 0.02 (Fig. 1*P*). Values in the terminal segments were (spines/μm): wild type, 0.83 ± 0.04; heterozygous, 0.38 ± 0.03; and mutant, 0.31 ± 0.02 (supplemental Fig. 1*D*, available at www.j-neurosci.org as supplemental material). This deficit cannot be attributed to neuronal ectopia because neurons were normally positioned in *reeler* heterozygous mice. We also analyzed apical dendrites in older (P32) mice. The data indicate that spine density is also drastically reduced in both heterozygous and homozygous *reeler* mice at this age in second- to fourth-order apical branches (Fig. 1*Q*), as well as terminals (supplemental Fig. 1*E*, available at www.jneurosci.org as supplemental material). These data demonstrate that normal levels of Reelin are required in the adult brain for the development or the maintenance of hippocampal dendritic spines.

To gain biochemical evidence of spine abnormalities, we also analyzed the expression of proteins normally associated with these structures in the *reeler* background. We first prepared total hippocampal protein extracts and crude synaptosomal fractions from adult wild-type mice and verified by Western blot analysis that the synaptosomal fractions were enriched, as expected, for presynaptic proteins such as synapsin IIA, and postsynaptic markers such as PSD-95 and the NMDA receptor subunit NR2A (Fig. 2*A*). These latter proteins have been previously shown to associate with the Reelin receptor ApoER2 in postsynaptic density fractions (Beffert et al., 2005). We then prepared lysates and crude synaptosomal fractions from the hippocampi of wild-type, heterozygous, and homozygous *reeler* littermates. Western blot analysis of total lysates revealed that the levels of NR2A and PSD-95 were similar in all genotypes (Fig. 2*B,C*). However, when synaptosomal fractions were analyzed, we found that the levels of NR2A and PSD-95 were significantly decreased in heterozygous
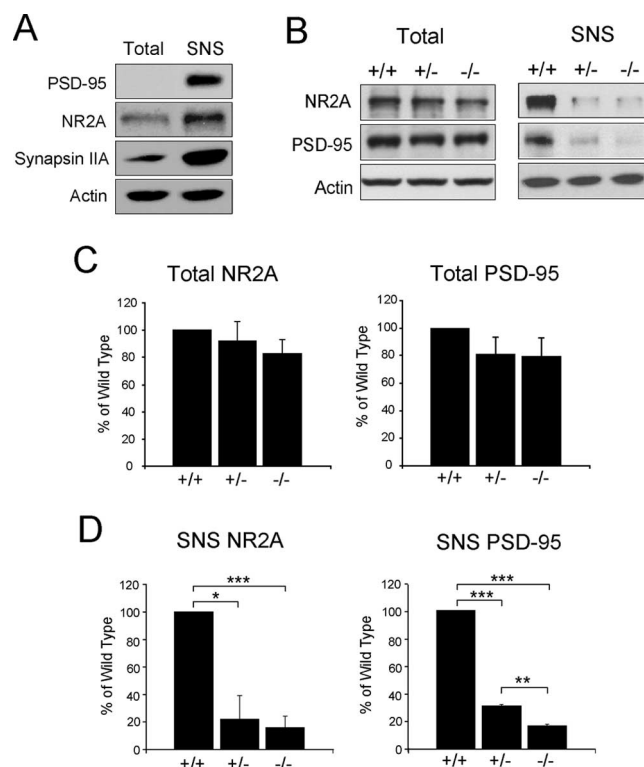

Figure 2. Reduced expression and synaptic localization of postsynaptic proteins in the hippocampus of heterozygous and homozygous *reeler* mice. *A*, Western blot analysis of presynaptic and postsynaptic proteins in total extracts and crude synaptosomal (SNS) fractions of wild-type mouse hippocampus. Postsynaptic proteins PSD-95 and NR2A, and the presynaptic protein synapsin IIA, are enriched in SNS fractions. Blots were reprobed with actin antibodies as a protein-loading control. *B*, Western blot analysis of postsynaptic proteins in total extracts and SNS fractions of wild-type, heterozygous, and homozygous *reeler* hippocampi. Quantification of the data is from triplicate experiments. *C, D*, Total levels of NR2A and PSD-95 are similar (*C*), whereas SNS levels (*D*) are significantly reduced in heterozygous and homozygous *reeler* mice compared with wild type.

and homozygous *reeler* mice compared with wild-type littermates (Fig. 2*B,D*). Levels of NR2A were 22 ± 17% in heterozygous (78% reduction from wild type) and 16 ± 8.3% in homozygous *reeler* mice (84% reduction from wild type). Levels of PSD-95 were 30.7 ± 1.3% in heterozygous (69.3% reduction from wild type) and 16.3 ± 1.5% in homozygous *reeler* mice (83.7% reduction from wild type). These observations further indicate that Reelin deficiency leads to the failed development or maintenance of dendritic spines.

Recombinant Reelin rescues the dendritic spine deficit in mutant *reeler* hippocampal organotypic cultures

To further investigate the role of Reelin in spine formation in an *in vitro* system that could be experimentally manipulated, we generated hippocampal organotypic cultures from littermates of the *reeler-YFP* mouse line. The cultures were routinely established at postnatal day 4 and maintained for 11 DIV to allow neuronal maturation to take place. When cultures were fixed and imaged, YFP-positive pyramidal neurons appeared arranged in a diffuse cellular layer in slice cultures obtained from wild-type (Fig. 3*A*) or heterozygous (data not shown) *reeler* mice, whereas they appeared clustered and disorganized in slices derived from homozygous *reeler* mutants (Fig. 3*C*). Immunofluorescence analysis confirmed that Reelin was abundantly expressed in Cajal-Retzius cells located in the SLM at the border between the hippocampus proper and the dentate gyrus (Fig. 3*B*), as it is
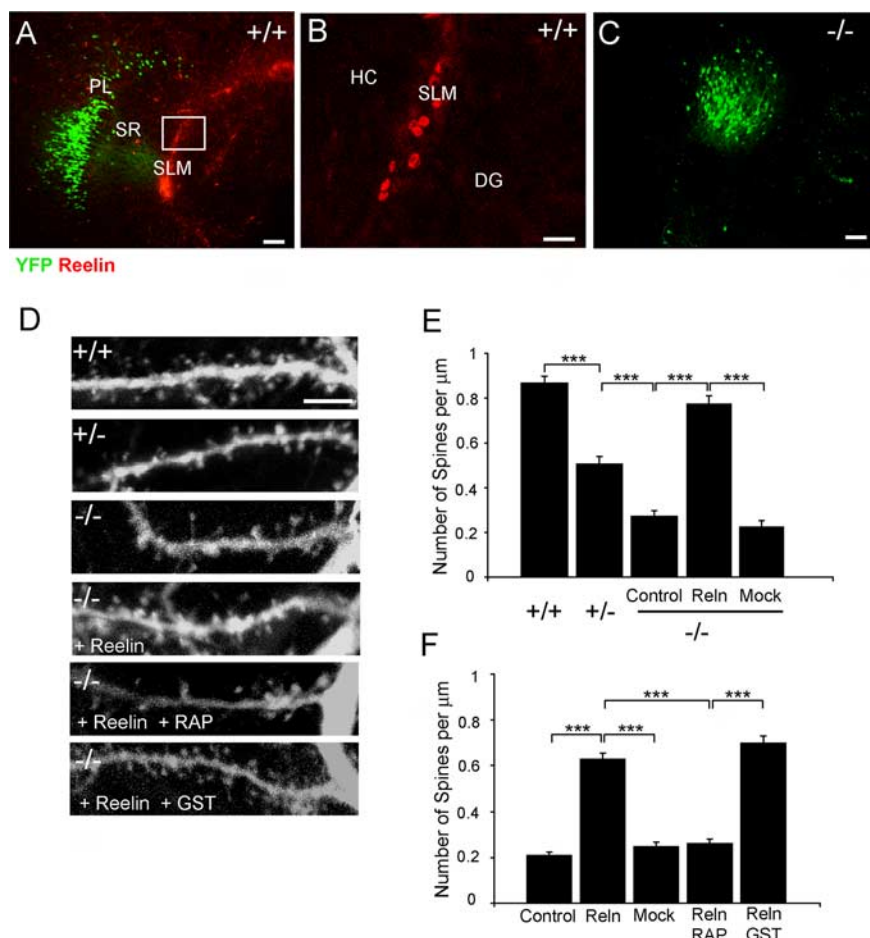
Figure 3. Reelin rescues the dendritic spine density deficit in *reeler* hippocampal slice cultures in a manner that is dependent on the activity of lipoprotein receptors. *A–C*, Double labeling of organotypic slice cultures obtained from YFP-positive wild-type or homozygous *reeler* hippocampi. Direct YFP fluorescence (green) and Reelin immunofluorescence (red) are shown. *B* is an enlargement of the boxed area in *A*. Reelin is expressed by Cajal-Retzius cells in the SLM. PL, pyramidal layer; HC, hippocampus proper; DG, dentate gyrus. Scale bars: *A, C*, 100 μm; *B*, 20 μm. *D*, Representative confocal images of second-order apical dendrite branches of CA1 pyramidal neurons in hippocampal cultures obtained from wild-type, heterozygous, or homozygous *reeler* mice and treated as indicated. More mature spines are present in wild-type cultures and in mutant cultures treated with Reelin and Reelin plus control GST, but not Reelin plus RAP. Scale bars, 5 μm. *E*, Quantification of spine density in second- to fourth-order apical dendrite branches in wild-type, heterozygous, or homozygous *reeler* hippocampal slice cultures. Spine density is significantly reduced in heterozygous and homozygous *reeler* compared with wild-type cultures. Spine density is significantly increased in mutant cultures treated with Reelin compared with mock-treated or untreated (control) slices. *F*, Quantification of spine density in second- to fourth-order apical dendrite branches from homozygous *reeler* hippocampal slices left untreated (control), treated with Reelin-conditioned medium, mock medium, Reelin plus RAP, or Reelin plus GST control. $n = 20–35$ dendrite segments per genotype or treatment from three independent experiments. Bar graphs (*E, F*) show the mean ± SEM; ***$p < 0.001$.

normally observed *in vivo*. Confocal analysis of dendritic branches (Fig. 3*D*) and terminals (supplemental Fig. 1*F*, available at www.jneurosci.org as supplemental material) indicated that mature spines were present in explants of all genotypes, but that spine density was strongly affected by the *Reelin* mutation. Quantitative analysis (Fig. 3*E*) demonstrated a dramatic reduction in spine density on apical dendrites of heterozygous and homozygous *reeler* mice, similar to the *in vivo* results described above. Values in apical branches were (spines/μm): wild type, 0.867 ± 0.03; heterozygous, 0.507 ± 0.034 (42% reduction compared with wild type); and homozygous *reeler* mice, 0.272 ± 0.026 (~69% reduction compared with wild type). Values in apical terminals were (spines/μm): wild type, 0.738 ± 0.032; heterozygous, 0.352 ± 0.018 (52% reduction compared with wild type); and homozygous *reeler* mice, 0.286 ± 0.018 (~61% reduction compared with wild type).

To determine whether Reelin directly promotes the formation of dendritic spines, cultured slices obtained from mutant *reeler* hippocampus were incubated continuously with a conditioned medium containing recombinant Reelin or with a mock medium for 10 DIV. The data show that Reelin treatment rescued the *reeler* phenotype and led to a significant increase in the density of dendritic spines compared with untreated explants or to cultures treated with mock medium (Fig. 3*D, E*). Densities in apical branches were 0.75 ± 0.04 spine/μm in Reelin-treated explants and 0.22 ± 0.03 spine/μm in mock-treated explants. Densities in terminal branches (supplemental Fig. 1*G*, available at www.jneurosci.org as supplemental material) were 0.69 ± 0.05 spine/μm in Reelin-treated explants and 0.24 ± 0.02 spine/μm in mock-treated explants. The difference between Reelin and mock values was statistically significant ($p < 0.001$) in both branches and terminals. The density value achieved in *reeler* explants cultured in the presence of Reelin was similar to that of wild-type cultures. These findings suggest that the observed reduced density of dendritic spines in heterozygous and homozygous mutant *reeler* mice is directly caused by Reelin deficiency *in vivo* and *in vitro*.

ApoER2 and VLDLR are required for Reelin-induced spine formation

High-affinity Reelin receptors of the lipoprotein receptor superfamily, ApoER2 and VLDLR, are expressed in hippocampal pyramidal neurons (Niu et al., 2004). To determine whether their binding activity is necessary for Reelin-induced spine development, we prepared sister hippocampal organotypic cultures from mutant *reeler* mice and incubated them with Reelin in the presence or absence of the competitive antagonist RAP fused to GST. This protein is well known to inhibit Reelin binding to ApoER2 and VLDLR, and to prevent Dab1 phosphorylation (Hiesberger et al., 1999). As a control we used GST alone or a mock conditioned medium. As above, Reelin treatment alone increased spine density in apical branches (Fig. 3*F*) as well as terminal dendrites (supplemental Fig. 1*G*, available at www.jneurosci.org as supplemental material) by ~3-fold compared with untreated control or mock treatment. Spine densities in apical branches of *reeler* explants were as follows: 0.63 ± 0.03 spine/μm in Reelin-treated explants, 0.25 ± 0.02 spine/μm in mock-treated explants, and 0.21 ± 0.01 spine/μm in untreated explants. Densities in terminal branches of *reeler* explants were as follows: 0.68 ± 0.02 spine/μm in Reelin-treated explants, 0.18 ± 0.02 spine/μm in mock-treated explants, and 0.26 ± 0.02 spine/μm in untreated explants. However, the addition of RAP completely prevented Reelin induction and resulted in spine density values similar to those observed in control

explants, whereas GST had no effect (Fig. 3 *D*,*F*). Apical branches of Reelin + RAP-treated explants had a density of 0.25 ± 0.02 spine/μm, whereas Reelin + GST-treated explants had a density of 0.70 ± 0.03 spine/μm. Terminal branches (supplemental Fig. 1*G*, available at www.jneurosci.org as supplemental material) of Reelin + RAP-treated explants had a density of 0.26 ± 0.02 spine/μm, whereas Reelin + GST-treated explants had a density of 0.68 ± 0.03 spine/μm. The difference between Reelin + RAP and Reelin alone or Reelin + GST was statistically significant ($p < 0.001$). These results strongly suggest that Reelin binding to VLDLR and ApoER2 is necessary to promote the formation of dendritic spines.

Dab1 is necessary for the acquisition of a normal spine density

Dab1 is a cytoplasmic adapter protein that binds to VLDLR and ApoER2 and mediates Reelin signaling (Hiesberger et al., 1999; Howell et al., 1999). The phenotype of *Dab1* homozygous null mutants is virtually indistinguishable from *reeler*, and is characterized by extensive neuronal ectopia (Howell et al., 1997). Like heterozygous *reeler*, heterozygous *Dab1* mutants exhibit no dyslamination of cellular layers. To investigate the role of Dab1 in spine formation, we generated a *Dab1* knockout-*YFP* mouse colony as described above for *reeler* mice, and obtained YFP-positive mice of all possible *Dab1* genotypes. Immunofluorescence analysis of hippocampal sections revealed that Dab1 is detectable in hippocampal pyramidal neurons,

Figure 4. Dendritic spine density is reduced in hippocampal pyramidal neurons of heterozygous and homozygous *Dab1*KO-*YFP* mice. *A–E*, Double labeling of YFP (green) and Dab1 (red) immunoreactivity in hippocampal sections from wild-type (*A–D*) and homozygous *Dab1* knock-out mice (*E*). Images in *B–D* are enlargements of the boxed area in *A*. Dab1 is expressed in YFP-positive pyramidal neurons in wild-type hippocampus. PL, pyramidal layer; HC, hippocampus proper; DG, dentate gyrus. Scale bars: *A*, *E*, 100 μm. *F–H*, Low-magnification confocal images of the hippocampus of adult YFP-positive wild-type, heterozygous, or homozygous *Dab1*KO-YFP littermates. YFP-positive neurons are ectopic in homozygous *Dab1* knock-out mice. Scale bars, 200 μm. *I–K*, Representative images of second-order apical dendrite branches of YFP-positive CA1 pyramidal neurons. Mature spines are present in all genotypes. Scale bars, 5 μm. *L*, Quantification of spine density in second- to fourth-order apical dendrite branches. Spine density is significantly reduced in heterozygous and homozygous *Dab1* knock-out compared with wild-type mice. *n* = 25 dendrite segments per genotype from three independent experiments. Bar graphs show the mean ± SEM; ****p* < 0.001.

including YFP-positive neurons, in wild-type, but not in knockout mutant mice (Fig. 4*A–E*). As expected, YFP-positive neurons were properly positioned in wild-type and heterozygous *Dab1* mice, and appeared ectopic in homozygous knock-out mutants (Fig. 4*F–H*). Next, we examined dendritic spines present on YFP-labeled apical branches (Fig. 4*I–K*) and terminals (supplemental Fig. 2*A–C*, available at www.jneurosci.org as supplemental material) of CA1 pyramidal neurons. As in *reeler*, quantitative analysis revealed that the density of dendritic spines is significantly reduced in heterozygous as well as homozygous *Dab1* mutants compared with wild-type littermates (Fig. 4*L*; supplemental Fig. 2*D*, available at www.jneurosci.org as supplemental material). Densities in apical dendritic branches were as follows (spines/μm): wild type, 0.75 ± 0.06; heterozygous, 0.47 ± 0.03; and mutant, 0.34 ± 0.03. Densities in terminal branches were as follows (spines/μm): wild type, 0.76 ± 0.03; heterozygous, 0.35 ± 0.02; and mutant, 0.41 ± 0.03. The difference between heterozygous or mutant and wild-type mice was statistically significant for both branches and terminals ($p < 0.001$).

To determine whether the expression and the recruitment of postsynaptic proteins to the spines are also affected by the *Dab1* genotype, we performed Western blot analysis of total hippocampal lysates and crude synaptosomal fractions. The data indicate
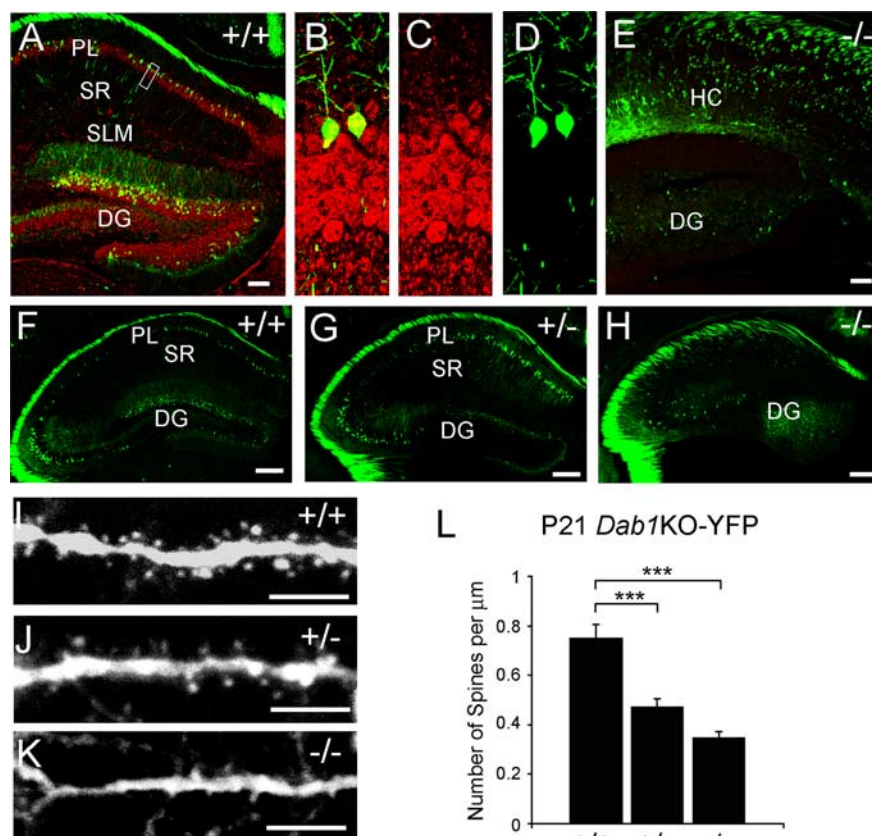
that, as in *reeler* mice, the total levels of NR2A and PSD-95 in hippocampal extracts did not significantly change in heterozygous or homozygous *Dab1* mutants compared with wild-type littermates (Fig. 5*A*). However, as in *reeler*, levels of NR2A and PSD-95 in synaptosomal preparations were significantly reduced in both heterozygous and homozygous *Dab1* mutants compared with wild type (Fig. 5*B*). Noticeably, however, the levels of NR2A in heterozygous *Dab1* knock-out mice were intermediate between those of wild-type and homozygous mice, whereas the levels of PSD-95 were similarly reduced in both heterozygous and homozygous *Dab1* mutants. Levels of NR2A were 66 ± 5.7% in heterozygous (34% reduction from wild type) and 15 ± 3.6% in homozygous *Dab1* mutant mice (85% reduction from wild type). Levels of PSD-95 were 33 ± 4.8% in heterozygous (67% reduction from wild type) and 44 ± 8.6% in homozygous *Dab1* knockout mice (56% reduction from wild type). These data suggest that Dab1 activity primarily affects the intracellular localization of postsynaptic proteins.

To confirm our *in vivo* observation that spine density is reduced in *Dab1* mutant mice, we also established hippocampal organotypic cultures from YFP-positive wild-type, heterozygous, and homozygous *Dab1* knock-out mice (Fig. 5*A–C*) and examined dendritic spines in apical branches (Fig. 6*D*) and terminals
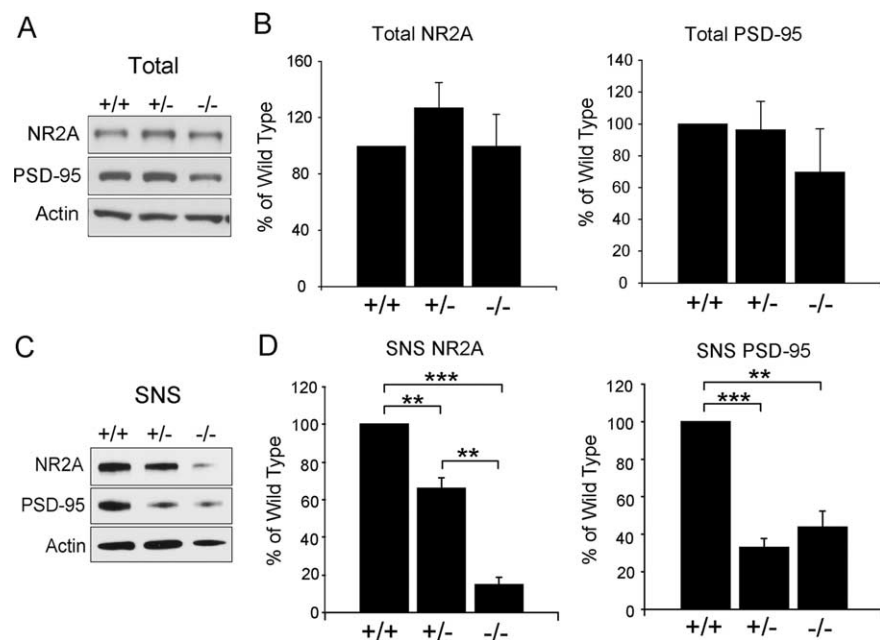
Figure 5. **A–D**, Reduced synaptic localization of postsynaptic proteins in the hippocampus of heterozygous and homozygous *Dab1*KO mice. Western blot analysis of postsynaptic proteins in total protein extracts (**A**) or synaptosomal (SNS) fractions (**C**) from the hippocampi of wild-type, heterozygous, and homozygous *Dab1* knock-out mice was performed. Blots were probed with NR2A and PSD-95 antibodies and, subsequently, with actin antibodies as a protein loading control. Quantification of the data was from three Western blot experiments. Total levels (**B**) of NR2A and PSD-95 were not significantly different. SNS levels (**D**) were significantly reduced in heterozygous and homozygous *Dab1* knock-out mice compared with wild-type littermates. Bar graphs show the mean ± SEM. **p < 0.01, ***p < 0.001.

(supplemental Fig. 2 *E*, available at www.jneurosci.org as supplemental material). Again, we observed a significant reduction in spine density in heterozygous and homozygous *Dab1* mutant cultures compared with wild type ($p < 0.001$). Densities in the apical branches were (spines/μm): wild type, 0.72 ± 0.04; heterozygous, 0.26 ± 0.03; and mutant 0.24 ± 0.03. Values in terminal branches were (spines/μm): wild type, 0.57 ± 0.05; heterozygous, 0.19 ± 0.02; and mutant, 0.08 ± 0.02. Thus, both *in vivo* and *in vitro* data indicate that Dab1 plays a role in dendritic spine formation.

Src family kinases are required for normal spine formation
Previous studies demonstrated that in order for Dab1 to transduce Reelin signaling, SFKs must phosphorylate it on specific tyrosine residues (Howell et al., 2000; Keshvara et al., 2001; Ballif et al., 2003). Addition of the specific SFK inhibitor PP2, but not the inert control compound PP3, blocks Reelin-induced Dab1 phosphorylation as well as the activation of downstream kinases such as Akt (Arnaud et al., 2003; Bock and Herz, 2003). We previously showed that PP2 also blocks Reelin-induced dendrite elongation in dissociated hippocampal neurons (Niu et al., 2004). Here, we used this pharmacological inhibitor to test the role of SFKs in dendritic spine formation using wild-type YFP-positive hippocampal cultures. Addition of PP2 at doses known to effectively block Dab1 phosphorylation resulted in a significant reduction of spine density in apical branches and terminals of pyramidal neurons compared with controls ($p < 0.001$), whereas PP3 had no effect (Fig. 6*E*; supplemental Fig. 2*F*, available at www.jneurosci.org as supplemental material). Densities in the apical branches of PP2-treated explants were 0.21 ± 0.01 spine/μm, those of PP3-treated explants were 0.64 ± 0.03 spine/μm, and those of untreated explants were 0.60 ± 0.03

spine/μm. Densities in the terminal branches were (spine/μm): PP2-treated explants, 0.17 ± 0.01; PP3-treated explants, 0.57 ± 0.03, and untreated explants, 0.53 ± 0.03. Together with the findings described above, these data indicate that Reelin-induced and SFK-mediated Dab1 phosphorylation is important for the formation or maintenance of dendritic spines.

Discussion
We investigated the role of Reelin signaling on dendritic spine formation, a prerequisite for synaptogenesis and the establishment of neuronal connectivity, and thus a crucial aspect of postnatal hippocampal development. We demonstrated that loss or reduction of Reelin signaling results in a dramatic defect in the density of dendritic spines in hippocampal pyramidal neurons *in vivo* and *in vitro*. Reduced spine density was observed in apical dendrites of heterozygous and homozygous mutant *reeler* mice (Figs. 1, 3). This phenotype is caused by a deficit in native Reelin, because it can be rescued *in vitro* by the addition of recombinant Reelin to the medium of *reeler* hippocampal cultures (Fig. 3). A similar phenotype consisting of reduced spine density was also seen in the hippocampus of *Dab1* heterozygous and homozygous knock-out mice *in vivo* and *in vitro* (Figs. 4, 6). Through the use of specific inhibitors, we further provided evidence that ApoER2 and VLDLR (Fig. 3) and SFKs (Fig. 6) are also crucial for the formation or maintenance of dendritic spines. It will be interesting in the future to investigate whether the PI3K/Akt/mTOR pathway, a downstream branch of the Reelin pathway that is important for dendrite growth (Jossin and Goffinet, 2007), also mediates its effect on spine development. Overall, our data highlight a biological function of the Reelin pathway in the postnatal brain, which affects neuronal maturation and enables the formation of normal circuitry in the mammalian brain.

We generated colonies of *reeler-YFP* or *Dab1* knock-out-*YFP* mice to better visualize hippocampal dendrites and spines. To expand on our *in vivo* observations, we established hippocampal cultures from these transgenic lines. YFP was detectable in many pyramidal and dentate neurons beginning at 2 DIV and remained cell type specific for the entire time in culture. Mature spines were observed starting at 5 DIV and continued to develop until at least 15 DIV. We selected 11 DIV as the most reliable time point when explants appeared healthy and mature spines could be observed and compared across different mutant genotypes. Our *in vitro* data are strikingly similar to those obtained *in vivo*, demonstrating a deficit in spine density in heterozygous or homozygous *reeler* and *Dab1* mutants. We also verified that organotypic cultures appropriately expressed Reelin mostly in Cajal-Retzius cells located at the boundary between the hippocampus proper and the dentate gyrus. These observations further indicate that the hippocampal organotypic culture is a valid model system to study Reelin-induced spine development.

Our findings are consistent with previous electron microscopy studies indicating that heterozygous *reeler* mice have fewer

spines than normal in the cortical gray matter (Liu et al., 2001) and that secreted Reelin accumulates in the extracellular matrix around dendrites and spines of cortical pyramidal neurons (Rodriguez et al., 2000). Given that at least some ApoER2 has also been localized to postsynaptic structures (Beffert et al., 2005), our data suggest that Reelin may act locally near synaptic contacts to promote spine development. However, it is also conceivable that Reelin affects spine development by acting remotely, in the cell body or in cellular processes to regulate the trafficking and localization of postsynaptic proteins at the synapse. Because postsynaptic proteins such as PSD-95 and the NMDA receptor interact with the ApoER2 (Beffert et al., 2005; Hoe et al., 2006), and Dab1 promotes membrane localization of Reelin receptors (Morimura et al., 2005), it is possible that changes in receptor trafficking in mutant mice may contribute to their reduction at the synapse. Alternatively, a specific defect in the trafficking of synaptic proteins and/or their assembly at the dendritic spines may underlie their deficit in Reelin signaling mutants. Further investigation will be necessary to elucidate the exact cause of the observed decrease of postsynaptic proteins in heterozygous and

Figure 6. Dab1 and SFK activity are required for the development of a normal dendritic spine density in organotypic hippocampal cultures. *A–C*, Organotypic cultures of the hippocampus of wild-type, heterozygous, and homozygous *Dab1*KO-*YFP* littermates. YFP-positive neurons are disorganized in the mutant cultures. PL, pyramidal layer. Scale bars, 100 μm. *D–E*, Quantification of spine density in second- to fourth-order apical dendrite branches in *Dab1*KO wild-type, heterozygous, or homozygous littermates (*D*) or branches of wild-type slice cultures treated with the PP2 SFK inhibitor or the inert control PP3 (*E*). Spine density is significantly reduced in heterozygous and homozygous *Dab1* knock-out compared with wild-type mice. $n = 19$–27 dendrite segments per genotype from three independent experiments. Spine density is also significantly decreased in PP2-treated cultures compared with controls. $n = 24$–30 dendrite segments per treatment from three independent experiments. Bar graphs show the mean $\pm$ SEM. ***$p < 0.001$.

mutant synaptosomal fractions. Noticeably, the decrease in synaptosomal levels of postsynaptic proteins in either heterozygous or homozygous mice was more dramatic compared with the decrease in spine density. This suggests that postsynaptic structures can form even in the presence of reduced levels of NR2A and PSD-95; however, it is possible that some of these spines may not be stable or may be unable to form active synapses. The static imaging technique used in this study does not allow us to determine whether the activity of Reelin induces the formation of new spines, promotes the maturation of immature spines, or favors the maintenance of mature spines at the sites of synaptic contact. Further studies using dynamic imaging techniques are necessary to address this issue.

The observed reduced density of spines seen in conditions in which the Reelin signaling pathway is suppressed may be viewed as the long-term result of poor dendrite development. Previous studies have in fact shown that dendrite development is impaired in young (3–5 DIV) hippocampal cultures of heterozygous or homozygous *reeler* mice. However, dendrite elongation in long-term cultures of Reelin signaling mutants appears normal (Maclaurin et al., 2007). In the present study we also found that the extension of apical dendrites is normal in heterozygous *reeler* mice examined at postnatal day 21 or 32, suggesting that the dendritic growth defect may be transient in mice with reduced Reelin activity, whereas the spine deficit may persist into adult ages.

In the past few years a number of studies focused on the role of Reelin in the postnatal and adult brain, particularly emphasizing its effect on synaptic transmission, plasticity, learning, and memory (for review, see Herz and Chen, 2006). Addition of recombinant Reelin promotes hippocampal long-term potentiation (LTP) through the activity of lipoprotein receptors (Weeber et al., 2002). A splicing variant of ApoER2 capable of interacting with PSD-95 and the JNK interacting protein is important for Reelin-induced
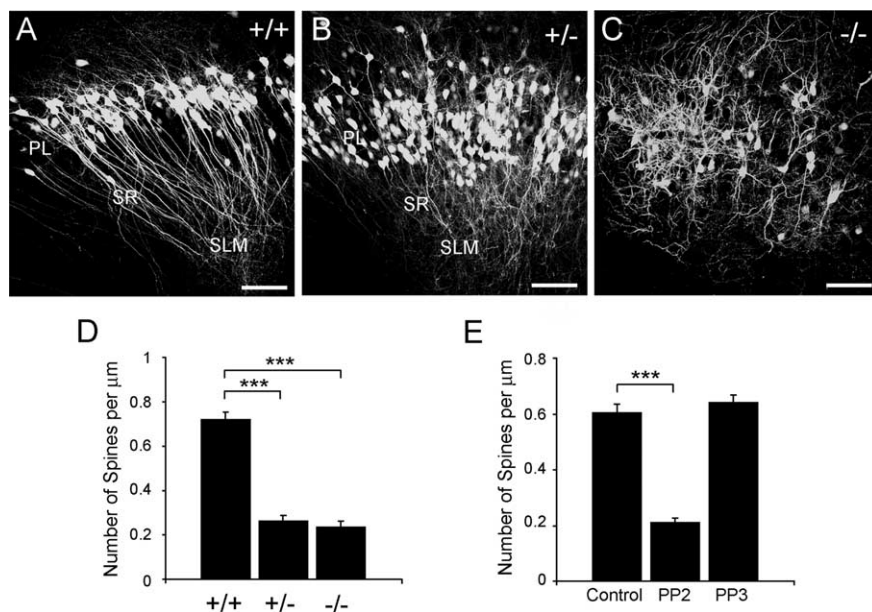
LTP and the formation of spatial memory (Beffert et al., 2005). The role of Reelin in synaptic function is mediated in part through interactions between ApoER2 and the NMDA receptor (Beffert et al., 2005). These proteins form a synaptic complex that controls Ca^{2+} entry and thus regulates synaptic plasticity. In addition, Reelin signaling is important for the regulation of NMDA receptor subunit composition during hippocampal maturation (Sinagra et al., 2005; Groc et al., 2007) and the NMDA receptor-mediated activity in cortical neurons (Chen et al., 2005). Recent studies further revealed that Reelin also enhances glutamatergic transmission through AMPA receptors (Qiu and Weeber, 2007). We further demonstrated here that Reelin, through the activation of its signaling pathway, impacts the recruitment of postsynaptic proteins to the spines, thus favoring the development of anatomical synaptic structures, in addition to impacting the physiological activity of the synapse.

Complete or partial loss of Reelin is associated with a variety of developmental brain disorders. Absence of Reelin attributable to genetic mutations results in lissencephaly with cerebellar hypoplasia (LCH), a phenotype similar to *reeler* characterized by severe and widespread neuronal migration defects (Hong et al., 2000). LCH patients also exhibit seizures, indicative of abnormal synaptic activity. Reduced *RELN* expression because of epigenetic mechanisms is associated with schizophrenia and psychotic bipolar disorder (Impagnatiello et al., 1998; Guidotti et al., 2000; Eastwood and Harrison, 2003; Grayson et al., 2005; Herz and Chen, 2006). Genetic association studies also supported an association of *RELN* gene variants with treatment-resistant schizophrenia (Goldberger et al., 2005), particularly in women (Shifman et al., 2008). A recent study further suggested that allelic variants of *RELN* contribute to specific endophenotypes of schizophrenia such as working memory and executive function-

ing (Wedenoja et al., 2008). Reduced Reelin expression was also reported in autistic patients (Fatemi et al., 2001). Genetic studies further supported a role for the *RELN* gene in the susceptibility to autism, at least in some populations (Persico et al., 2001; Zhang et al., 2002; Skaar et al., 2005; Serajee et al., 2006). Interestingly, we found that the spine density deficit is prominent in heterozygous *reeler* mice, in which reduced Reelin levels are present, and it is quite similar to that of homozygous mutants. This unexpected result is further corroborated by explant and Dab1 mutant anatomical data, and by biochemical data. Overall, the results suggest that the control of spine development by Reelin is independent of the regulation of neuronal positioning and further validate the use of heterozygous *reeler* mice as models of cognitive dysfunctions.

In addition to developmental brain disorders, Reelin has also been implicated in neurodegenerative diseases, suggesting a convergence of these two apparently distinct types of disorders (Bothwell and Giniger, 2000). Independent studies reported altered Reelin expression and glycosylation patterns (Botella-Lopez et al., 2006), and reductions of Reelin-expressing pyramidal neurons, in the entorhinal cortex of Alzheimer's disease brains (Chin et al., 2007). Whether developmental or degenerative in nature, cognitive disorders likely arise from abnormalities in synaptic connectivity or function. Our findings provide a plausible mechanism by which Reelin deficiency may be a potential risk factor for cognitive dysfunctions.

References

Alcántara S, Ruiz M, D'Arcangelo G, Ezan F, de Lecea L, Curran T, Sotelo C, Soriano E (1998) Regional and cellular patterns of *reelin* mRNA expression in the forebrain of the developing and adult mouse. J Neurosci 18:7779–7799.

Arnaud L, Ballif BA, Förster E, Cooper JA (2003) Fyn tyrosine kinase is a critical regulator of disabled-1 during brain development. Curr Biol 13:9–17.

Ballif BA, Arnaud L, Cooper JA (2003) Tyrosine phosphorylation of Disabled-1 is essential for Reelin-stimulated activation of Akt and Src family kinases. Brain Res Mol Brain Res 117:152–159.

Beffert U, Weeber EJ, Durudas A, Qiu S, Masiulis I, Sweatt JD, Li WP, Adelmann G, Frotscher M, Hammer RE, Herz J (2005) Modulation of synaptic plasticity and memory by Reelin involves differential splicing of the lipoprotein receptor ApoER2. Neuron 47:567–579.

Bock HH, Herz J (2003) Reelin activates SRC family tyrosine kinases in neurons. Curr Biol 13:18–26.

Borrell V, Del Rio JA, Alcántara S, Derer M, Martínez A, D'Arcangelo G, Nakajima K, Mikoshiba K, Derer P, Curran T, Soriano E (1999) Reelin regulates the development and synaptogenesis of the layer-specific entorhino-hippocampal connections. J Neurosci 19:1345–1358.

Botella-López A, Burgaya F, Gavin R, Garcia-Ayllón MS, Gómez-Tortosa E, Peña-Casanova J, Ureña JM, Del Rio JA, Blesa R, Soriano E, Sáez-Valero J (2006) Reelin expression and glycosylation patterns are altered in Alzheimer's disease. Proc Natl Acad Sci USA 103:5573–5578.

Bothwell M, Giniger E (2000) Alzheimer's disease: neurodevelopment converges with neurodegeneration. Cell 102:271–273.

Brigman JL, Padukiewicz KE, Sutherland ML, Rothblat LA (2006) Executive functions in the heterozygous reeler mouse model of schizophrenia. Behav Neurosci 120:984–988.

Chen Y, Beffert U, Ertunc M, Tang TS, Kavalali ET, Bezprozvanny I, Herz J (2005) Reelin modulates NMDA receptor activity in cortical neurons. J Neurosci 25:8209–8216.

Chin J, Massaro CM, Palop JJ, Thwin MT, Yu GQ, Bien-Ly N, Bender A, Mucke L (2007) Reelin depletion in the entorhinal cortex of human amyloid precursor protein transgenic mice and humans with Alzheimer's disease. J Neurosci 27:2727–2733.

Craig AM, Graf ER, Linhoff MW (2006) How to build a central synapse: clues from cell culture. Trends Neurosci 29:8–20.

D'Arcangelo G (2005) Apoer2: a Reelin receptor to remember. Neuron 47:471–473.

D'Arcangelo G (2006) Reelin mouse mutants as models of cortical development disorders. Epilepsy Behav 8:81–90.

D'Arcangelo G, Miao GG, Chen SC, Soares HD, Morgan JI, Curran T (1995) A protein related to extracellular matrix proteins deleted in the mouse mutant reeler. Nature 374:719–723.

Eastwood SL, Harrison PJ (2003) Interstitial white matter neurons express less reelin and are abnormally distributed in schizophrenia: towards an integration of molecular and morphologic aspects of the neurodevelopmental hypothesis. Mol Psychiatry 8:821–831.

Fatemi SH, Stary JM, Halt AR, Realmuto GR (2001) Dysregulation of Reelin and Bcl-2 proteins in autistic cerebellum. J Autism Dev Disord 31:529–535.

Feng G, Mellor RH, Bernstein M, Keller-Peck C, Nguyen QT, Wallace M, Nerbonne JM, Lichtman JW, Sanes JR (2000) Imaging neuronal subsets in transgenic mice expressing multiple spectral variants of GFP. Neuron 28:41–51.

Goldberger C, Gourion D, Leroy S, Schürhoff F, Bourdel MC, Leboyer M, Krebs MO (2005) Population-based and family-based association study of 5′UTR polymorphism of the reelin gene and schizophrenia. Am J Med Genet B Neuropsychiatr Genet 137:51–55.

Grayson DR, Jia X, Chen Y, Sharma RP, Mitchell CP, Guidotti A, Costa E (2005) Reelin promoter hypermethylation in schizophrenia. Proc Natl Acad Sci U S A 102:9341–9346.

Groc L, Choquet D, Stephenson FA, Verrier D, Manzoni OJ, Chavis P (2007) NMDA receptor surface trafficking and synaptic subunit composition are developmentally regulated by the extracellular matrix protein Reelin. J Neurosci 27:10165–10175.

Guidotti A, Auta J, Davis JM, Di-Giorgi-Gerevini V, Dwivedi Y, Grayson DR, Impagnatiello F, Pandey G, Pesold C, Sharma R, Uzunov D, Costa E (2000) Decrease in reelin and glutamic acid decarboxylase67 (GAD67) expression in schizophrenia and bipolar disorder: a postmortem brain study. Arch Gen Psychiatry 57:1061–1069.

Herz J, Chen Y (2006) Reelin, lipoprotein receptors and synaptic plasticity. Nat Rev Neurosci 7:850–859.

Hiesberger T, Trommsdorff M, Howell BW, Goffinet A, Mumby MC, Cooper JA, Herz J (1999) Direct binding of Reelin to VLDL receptor and ApoE receptor 2 induces tyrosine phosphorylation of Disabled-1 and modulates Tau phosphorylation. Neuron 24:481–489.

Hoe HS, Tran TS, Matsuoka Y, Howell BW, Rebeck GW (2006) DAB1 and Reelin effects on amyloid precursor protein and ApoE receptor 2 trafficking and processing. J Biol Chem 281:35176–35185.

Hong SE, Shugart YY, Huang DT, Al Shahwan S, Grant PE, Hourihane JO, Martin ND, Walsh CA (2000) Autosomal recessive lissencephaly with cerebellar hypoplasia is associated with human RELN mutations. Nat Genet 26:93–96.

Howell BW, Hawkes R, Soriano P, Cooper JA (1997) Neuronal position in the developing brain is regulated by mouse disabled-1. Nature 389:733–737.

Howell BW, Herrick TM, Cooper JA (1999) Reelin-induced tyrosine phosphorylation of Disabled 1 during neuronal positioning. Genes Dev 13:643–648.

Howell BW, Herrick TM, Hildebrand JD, Zhang Y, Cooper JA (2000) Dab1 tyrosine phosphorylation sites relay positional signals during mouse brain development. Curr Biol 10:877–885.

Impagnatiello F, Guidotti AR, Pesold C, Dwivedi Y, Caruncho H, Pisu MG, Uzunov DP, Smalheiser NR, Davis JM, Pandey GN, Pappas GD, Tueting P, Sharma RP, Costa E (1998) A decrease of reelin expression as a putative vulnerability factor in schizophrenia. Proc Natl Acad Sci USA 95:15718–15723.

Jossin Y, Goffinet AM (2007) Reelin Signals through Phosphatidylinositol 3-Kinase and Akt To Control Cortical Development and through mTor To Regulate Dendritic Growth. Mol Cell Biol 27:7113–7124.

Keshvara L, Benhayon D, Magdaleno S, Curran T (2001) Identification of reelin-induced sites of tyrosyl phosphorylation on disabled 1. J Biol Chem 276:16008–16014.

Krueger DD, Howell JL, Hebert BF, Olausson P, Taylor JR, Nairn AC (2006) Assessment of cognitive function in the heterozygous reeler mouse. Psychopharmacology (Berl) 189:95–104.

Kuo G, Arnaud L, Kronstad-O'Brien P, Cooper JA (2005) Absence of Fyn and Src causes a reeler-like phenotype. J Neurosci 25:8578–8586.

Lambert de Rouvroit C, Goffinet AM (1998) The reeler mouse as a model of brain development. Adv Anat Embryol Cell Biol 150:1–108.

Liu WS, Pesold C, Rodriguez MA, Carboni G, Auta J, Lacor P, Larson J, Condie BG, Guidotti A, Costa E (2001) Down-regulation of dendritic

spine and glutamic acid decarboxylase 67 expressions in the reelin haplo-insufficient heterozygous reeler mouse. Proc Natl Acad Sci U S A 98:3477–3482.

Maclaurin SA, Krucker T, Fish KN (2007) Hippocampal dendritic arbor growth in vitro: Regulation by Reelin-Disabled-1 signaling. Brain Res 1172:1–9.

Mariani J (1982) Extent of multiple innervation of Purkinje cells by climbing fibers in the olivocerebellar system of weaver, reeler and staggerer mutant mice. J Neurosci 13:119–126.

Morimura T, Hattori M, Ogawa M, Mikoshiba K (2005) Disabled1 regulates the intracellular trafficking of reelin receptors. J Biol Chem 280:16901–16908.

Niu S, Renfro A, Quattrocchi CC, Sheldon M, D'Arcangelo G (2004) Reelin promotes hippocampal dendrite development through the VLDLR/ApoER2-Dab1 pathway. Neuron 41:71–84.

Olson EC, Kim S, Walsh CA (2006) Impaired neuronal positioning and dendritogenesis in the neocortex after cell-autonomous Dab1 suppression. J Neurosci 26:1767–1775.

Persico AM, D'Agruma L, Maiorano N, Totaro A, Militerni R, Bravaccio C, Wassink TH, Schneider C, Melmed R, Trillo S, Montecchi F, Palermo M, Pascucci T, Puglisi-Allegra S, Reichelt KL, Conciatori M, Marino R, Quattrocchi CC, Baldi A, Zelante L, et al. (2001) Reelin gene alleles and haplotypes as a factor predisposing to autistic disorder. Mol Psychiatry 6:150–159.

Qiu S, Weeber EJ (2007) Reelin signaling facilitates maturation of CA1 glutamatergic synapses. J Neurophysiol 97:2312–2321.

Rice DS, Nusinowitz S, Azimi AM, Martínez A, Soriano E, Curran T (2001) The reelin pathway modulates the structure and function of retinal synaptic circuitry. Neuron 31:929–941.

Rodriguez MA, Pesold C, Liu WS, Kriho V, Guidotti A, Pappas GD, Costa E (2000) Colocalization of integrin receptors and reelin in dendritic spine postsynaptic densities of adult nonhuman primate cortex. Proc Natl Acad Sci U S A 97:3550–3555.

Serajee FJ, Zhong H, Mahbubul Huq AH (2006) Association of Reelin gene polymorphisms with autism. Genomics 87:75–83.

Sheldon M, Rice DS, D'Arcangelo G, Yoneshima H, Nakajima K, Mikoshiba K, Howell BW, Cooper JA, Goldowitz D, Curran T (1997) *Scrambler* and *yotari* disrupt the *disabled* gene and produce a *reeler*-like phenotype in mice. Nature 389:730–733.

Shifman S, Johannesson M, Bronstein M, Chen SX, Collier DA, Craddock NJ, Kendler KS, Li T, O'Donovan M, O'Neill FA, Owen MJ, Walsh D, Weinberger DR, Sun C, Flint J, Darvasi A (2008) A genome-wide association identifies a common variant in the reelin gene that increases the risk of schizophrenia only in women. PLoS Genet 4:e28.

Sinagra M, Verrier D, Frankova D, Korwek KM, Blahos J, Weeber EJ, Manzoni OJ, Chavis P (2005) Reelin, very-low-density lipoprotein receptor, and apolipoprotein E receptor 2 control somatic NMDA receptor composition during hippocampal maturation in vitro. J Neurosci 25:6127–6136.

Skaar DA, Shao Y, Haines JL, Stenger JE, Jaworski J, Martin ER, DeLong GR, Moore JH, McCauley JL, Sutcliffe JS, Ashley-Koch AE, Cuccaro ML, Folstein SE, Gilbert JR, Pericak-Vance MA (2005) Analysis of the RELN gene as a genetic risk factor for autism. Mol Psychiatry 10:563–571.

Stoppini L, Buchs PA, Muller D (1991) A simple method for organotypic cultures of nervous tissue. J Neurosci Methods 37:173–182.

Tabata H, Nakajima K (2002) Neurons tend to stop migration and differentiate along the cortical internal plexiform zones in the Reelin signal-deficient mice. J Neurosci Res 69:723–730.

Trommsdorff M, Gotthardt M, Hiesberger T, Shelton J, Stockinger W, Nimpf J, Hammer RE, Richardson JA, Herz J (1999) Reeler/Disabled-like disruption of neuronal migration in knockout mice lacking the VLDL receptor and ApoE receptor 2. Cell 97:689–701.

Tueting P, Costa E, Dwivedi Y, Guidotti A, Impagnatiello F, Manev R, Pesold C (1999) The phenotypic characteristics of heterozygous reeler mouse. Neuroreport 10:1329–1334.

Ware ML, Fox JW, González JL, Davis NM, Lambert de Rouvroit C, Russo CJ, Chua SC Jr, Goffinet AM, Walsh CA (1997) Aberrant splicing of a mouse *disabled* homolog, *mdab1*, in the *scrambler* mouse. Neuron 19:239–249.

Wedenoja J, Loukola A, Tuulio-Henriksson A, Paunio T, Ekelund J, Silander K, Varilo T, Heikkilä K, Suvisaari J, Partonen T, Lönnqvist J, Peltonen L (2008) Replication of linkage on chromosome 7q22 and association of the regional Reelin gene with working memory in schizophrenia families. Mol Psychiatry 13:673–684.

Weeber EJ, Beffert U, Jones C, Christian JM, Forster E, Sweatt JD, Herz J (2002) Reelin and ApoE receptors cooperate to enhance hippocampal synaptic plasticity and learning. J Biol Chem 277:39944–39952.

Zhang H, Liu X, Zhang C, Mundo E, Macciardi F, Grayson DR, Guidotti AR, Holden JJ (2002) Reelin gene alleles and susceptibility to autism spectrum disorders. Mol Psychiatry 7:1012–1017.